This article has been accepted for publication in a future issue of this journal, but has not been fully edited. Content may change prior to final publication. Citation information: DOI 10.1109/JIOT.2018.2816597, IEEE Internet of Things Journal

Energy-Efficient User Scheduling and Power Allocation for NOMA based Wireless Networks with Massive IoT Devices

Daosen Zhai, Ruonan Zhang, *Member, IEEE,* Lin Cai, *Senior Member, IEEE,* Bin Li, *Member, IEEE,* and Yi Jiang

***Abstract*—Non-Orthogonal Multiple Access (NOMA) exhibits superiority in spectrum efficiency and device connections in comparison with the traditional orthogonal multiple access technologies. However, the non-orthogonality of NOMA also introduces intra-cell interference that has become the bottleneck limiting the performance to be further improved. To coordinate the intra-cell interference, we investigate the dynamic user scheduling and power allocation problem in this paper. Specifically, we formulate this problem as a stochastic optimization problem with the objective to minimize the total power consumption of the whole network under the constraint of all users' long-term rate requirements. To tackle this challenging problem, we first transform it into a series of static optimization problems based on the stochastic optimization theory. Afterward, we exploit the special structure of the reformulated problem and adopt the branch-and-bound technique to devise an efficient algorithm, which can obtain the optimal control policies with a low complexity. As a good feature, the proposed algorithm can make decisions only according to the instantaneous system state and can guarantee the long-term network performance. Simulation results demonstrate that the proposed algorithm has good performance in convergence and outperforms other schemes in terms of power consumption and user satisfaction.**

I. Introduction

The fifth generation mobile communication systems (5G) will penetrate into every element of future society such that a unified wireless network connecting everything will be created. At the same time, several serious challenges are also posed for 5G, such as the requirements for one million connections per km^2, millisecond end-to-end latency, Gbps user experienced data rate, and more severe physical layer security [1], [2]. To meet these rigorous requirements, ten key wireless technologies are presented in the 5G white paper on wireless technology architecture [3]. As indicated in the white paper, non-orthogonal multiple access (NOMA) is a potential candidate for the air interface techniques of 5G. Furthermore, note that a downlink version of NOMA, i.e., multiuser superposition transmission (MUST), has been proposed in Third Generation Partnership Project (3GPP) Long Term Evolution (LTE) Release-13 [4].

In NOMA systems, multiuser superposition coding is implemented in transmitters and successive interference cancellation (SIC) is adopted at receivers so that the receivers can recover their desired information from the multiplexed signals. Exploiting user diversities in power domain, NOMA is capable of accommodating more users on the same spectrum in comparison with the traditional orthogonal multiple access technologies. It has been verified in both theory [5] and system-level simulations [6] that NOMA outperforms orthogonal frequency-division multiple access (OFDMA) in terms of spectrum efficiency and device connections. Therefore, NOMA is very suitable for the 5G application scenarios of ultra-low latency and ultra-high connectivity [7], e.g., the Internet of Things (IoT) in urban areas [8].

A. Motivations

Notwithstanding the above benefits, NOMA also has some shortcomings. First of all, the multiuser detection method SIC increases the decoding complexity of receivers, which is a heavy burden on the computing ability and battery capacity constrained mobile devices. Furthermore, the non-orthogonality of NOMA leads to intra-cell interference that becomes the bottleneck to further upgrade the performance. To overcome these shortcomings and promote the application of NOMA in 5G-based IoT, extensive works have been conducted for NOMA systems in recent years. In order to reduce the decoding complexity, some approaches have been proposed in [9]–[13], including new detection algorithms [9], [10], efficient coded modulation [11], [12], and some of the approximation methods [13]. To coordinate the intra-cell interference and further enhance the performance of NOMA networks, abundant control policies have been devised, including power allocation [14]–[16], channel assignment [17]–[22], user pairing (or clustering) [23]–[25], rate control [26], [27], etc.

Although the existing works have enhanced the performance of NOMA networks to some extent, they still have some limits. As a common feature, all works in [14]–[27] make an implicit assumption that the network can support the connectivity of all users at the same time. However, it is almost impossible for the future networks to meet this special requirement especially for

This work was supported by the National Natural Science Foundation of China (Grant No. 61571370 and 61601365), Natural Science Basic Research Plan in Shaanxi Province (No. 2016JQ6017) , National Science and Technology Major Project under Grant 2016ZX03001015, Fundamental Research Funds for the Central Universities (Grant No. 3102017OQD091 and 3102017GX08003), and NSERC. *(Corresponding author: Ruonan Zhang)*

Daosen Zhai, Ruonan Zhang, Bin Li, and Yi Jiang are with School of Electronics and Information, Northwestern Polytechnical University, Xi'an, Shaanxi, 710072, China (e-mail: zhaidaosen@nwpu.edu.cn; rzhang@nwpu.edu.cn; libin@nwpu.edu.cn; jiangyiv88@nwpu.edu.cn).

L. Cai is with the Department of Electrical and Computer Engineering, University of Victoria, Victoria, BC V8P 5C2, Canada (e-mail: cai@ece.uvic.ca).

This article has been accepted for publication in a future issue of this journal, but has not been fully edited. Content may change prior to final publication. Citation information: DOI 10.1109/JIOT.2018.2816597, IEEE Internet of Things Journal

the scenario with massive connections (e.g., IoT that connects a very large number of devices but usually with a small data rate requirement). For this condition, user scheduling in the time domain should be adopted so as to satisfy the quality-of-services (QoS) of all users. Although there have been some works studying on the user scheduling problem [28]–[32], they usually focus on the instantaneous network performance by scheduling partial users, and thus the QoS of all users cannot be guaranteed. Furthermore, appropriate user scheduling can schedule the users with distinct channel conditions in the same time slot while the others with similar channel conditions in different slots, which is more helpful for developing the near-far effect of users. Moreover, serving many users at the same time and frequency will greatly increase the decoding complexity that is intolerable for mobile devices as discussed earlier. Therefore, it is necessary to design appropriate user scheduling strategies for NOMA networks.

B. Contributions

Motivated by the above reasons, we in this paper investigate the dynamic user scheduling and power allocation problem for NOMA based downlink networks with massive IoT devices. The main contributions of this paper are summarized as follows.

- We formulate the joint user scheduling and power allocation problem as a stochastic optimization problem with the objective to minimize the long-term power consumption of the whole system including the base station and all mobile devices. Specifically, the discontinuous reception mode is considered for mobile devices, that is, during the unscheduled period, the mobile devices can sleep for energy conservation. This energy saving approach is in favor of prolonging the standby time of the energy constrained devices such as sensor nodes or wearable devices. Besides, the long-term rate requirements of all users are also considered as constraints in the problem formulation, such that the QoS of all users can be guaranteed.
- We devise a dynamic user scheduling and power allocation algorithm (DUSPA) based on the Lyapunov optimization technique. Particularly, the DUSPA is an online algorithm that can make decisions without requiring any statistical information about the random channel conditions. Besides, we proof that the long-term rate requirements of all users can be strictly guaranteed by the proposed DUSPA. However, a mixed integer and non-convex programming (MINCP) is embedded in the DUSPA and should be solved optimally. To overcome this difficulty, we first transform the MINCP into a tractable one by theoretical analysis. Afterward, exploiting the special structure of the transformed problem, we employ the branch-and-bound framework to devise a low-complexity algorithm to obtain the optimal user scheduling and power allocation policies in each slot.
- We present extensive simulation results to evaluate the performance of the proposed algorithm. It shows that the DUSPA can converge to a balance point which makes a tradeoff between the total power consumption and the virtual queue backlog. Furthermore, it is also verified that the rate requirements of all users can be satisfied by the DUSPA. Moreover, comparing to other schemes, simulation results demonstrate that the proposed algorithm can save more power in underloaded systems and provide better user satisfaction in overloaded systems. Last, we reveal that the optimal number of users scheduled on each time-frequency resource for energy conservation is about 2-3, which is a helpful guidance for the design of practical NOMA networks.

C. Organization

The remainder of this paper is organized as follows. In section II, we demonstrate the details of related works. Section III introduces the network model and the problem formulation. In section IV, we elaborate the proposed algorithm DUSPA. Section V describes the algorithm design for the instantaneous resource management problem embedded in the DUSPA. Simulation results are presented in section VI. Finally, we conclude our paper in Section VII.

II. Related Work

In this section, we introduce the details of the related works. As the decoding complexity problem is not the primary concern of this paper, the detailed introduction for the related works [9]–[13] is omitted for brevity. In what follows, we concentrate on introducing the researches on how to deal with the intra-cell interference in NOMA networks.

To coordinate the intra-cell interference, abundant control policies have been devised in recent years, including power allocation [14]–[16], channel assignment [17]–[22], user pairing (or clustering) [23]–[25], rate control [26], [27], etc. In detail, a general power allocation scheme was proposed in [14] for both uplink and downlink networks to realize different tradeoff between user fairness and system throughput. Focusing on the downlink transmission, the authors in [15] analytically obtained the closed-form or semi-closed solutions to the power optimization problems with different criteria. Different from [14] and [15], [16] considered the MIMO-NOMA systems with a layered transmission scheme and designed the corresponding power allocation algorithm. With channel assignment taken into account, [17] proposed an iterative resource allocation algorithm to maximize the weighted sum-rate. Using a different approach, [18] devised a maximum weighted independent set based resource allocation algorithm for uplink networks. Besides, the energy-efficient channel assignment and power allocation algorithms were designed for NOMA networks with perfect [19], [20] and imperfect channel conditions [21]. From the perspective of mathematical analysis, [22] characterized the tractability of the joint problem under a range of constraints and utility functions. In addition, the user pairing and power allocation problem was studied in [23]–[25] and the joint rate and power control problem was investigated in [26], [27].

As a common feature, all works in [14]–[27] make an implicit assumption that the network can support the connectivity

This article has been accepted for publication in a future issue of this journal, but has not been fully edited. Content may change prior to final publication. Citation information: DOI 10.1109/JIOT.2018.2816597, IEEE Internet of Things Journal

of all users at the same time. However, when the number of users is much larger than the communication resources of the network as the IoT system that connects massive devices, the control policies proposed in [14]–[27] cannot work. To deal with this problem, the schemes of user scheduling in the time domain have been studied in [28]–[32]. Specifically, the uplink user scheduling problem was investigated in [28], the objective of which is to either maximize the throughput of the system or to obtain some kind of fairness among the users. In [29], the authors proposed a joint subcarrier and transmission power allocation algorithm to maximize the connectivity for narrow-band IoT systems [33] with NOMA. The proportional fair scheduling problem was studied in [30] by jointly considering the user selection and utility maximization problems. A hybrid reservation/contention-based medium access control protocol was designed in [31] to achieve the goal of adaptive user scheduling and thus higher multiplexing gain. In [32], a multi-dimensional tuple-link based model was adopted to devise a joint scheduling and resource allocation scheme. Although the works in [28]–[32] have studied the user scheduling problems, they usually focus on the instantaneous network performance by scheduling partial users, and thus the QoS of all users cannot be strictly guaranteed. To satisfy the QoS of all users, the dynamic user scheduling strategies for NOMA networks should be carefully designed, which motivates the work of this paper.

III. Network Model and Problem Formulation

In this section, we first introduce the concerned network model and definitions. Then, we present the problem formulation.

A. Network Model

As shown in Fig. 1, we consider a NOMA based downlink network, which consists of one base station (BS) and M IoT mobile devices (MDs). For notational simplicity, the set of MDs is represented by $\mathcal{U}$, i.e., $\mathcal{U} = \{1, 2, \cdots, M\}$. Besides, the network is assumed to operate in slotted time with slots normalized to integral units, and slot t refers to the time interval $[t, t+1)$, $t \in \{0, 1, 2, \cdots\}$. In slot t, the channel power gain (CPG) from the BS to MD m is denoted by $g_m(t)$, which accounts for the pass loss, shadowing, and fading. In addition, we consider the block fading channel model[1], that is, $g_m(t)$ remains constant during one slot, but may change on slot boundaries. For simplicity of expression, all MDs are sorted in the ascending order of their CPG (i.e., $g_i(t) < g_j(t), \forall i < j$). It is worth noting that the order of MDs is not fixed. With the dynamic change of the channel conditions $\mathcal{G}(t) = \{g_m(t)\}$, the order of MDs among different time slots may change as well.

In NOMA networks, the BS can simultaneously transmit data to multiple MDs on the same spectrum via superposition coding. To fully exploit the near-far effect of users and control the decoding complexity, we jointly consider the user scheduling and power allocation for NOMA networks, as depicted in Fig. 1. To model the control policy, we define $\mathcal{P}(t) = \{p_m(t)\}$ and $\mathcal{A}(t) = \{a_m(t)\}$ as the power allocation variables and the user scheduling variables, respectively. More specifically, in $\mathcal{P}(t) = \{p_m(t)\}$, $p_m(t)$ represents the transmit power allocated by the BS to MD m. In $\mathcal{A}(t) = \{a_m(t)\}$, $a_m(t) = 1$ if MD m is scheduled in slot t; otherwise $a_m(t) = 0$. In the scheduled slots, the relevant MDs must keep the status of data reception, which leads to some power consumption. The consumed power of MD m due to data reception is denoted by p_m^c. In the unscheduled slots, the relevant MDs can turn off the corresponding circuits [36], which is in favor of energy conservation especially for the enery-constrained IoT devices. This energy-saving mode is in accordance with the Discontinuous Reception (DRX) [37].

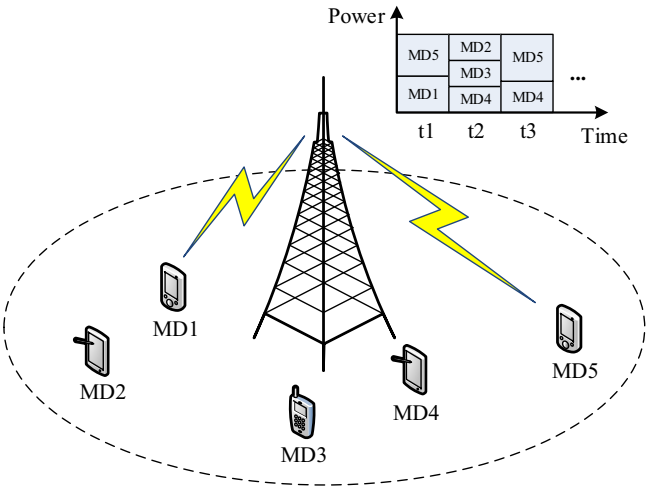

Figure 1. The scenario of a downlink NOMA wireless network with joint user scheduling and power allocation.

At the receiver side, the MDs can successfully decode their desired signals through successive SIC. According to [17], [19], the optimal decoding order in the downlink transmission should be in the ascending order in the CPG[2]. As such, the MDs with larger CPG will cause interference to the MDs with smaller CPG, rather than vice versa. Therefore, the signal-to-interference-plus-noise ratio (SINR) of MD m can be written as

$$\gamma_m(t) = \frac{p_m(t) g_m(t)}{\sum\limits_{i \in \mathcal{U}, i > m} p_i(t) g_m(t) + \sigma^2}, \tag{1}$$

where σ^2 is the additive white Gaussian noise.

According to the Shannon equation, the achievable data rate of MD m in slot t can be expressed as

$$R_m(t) = a_m(t) B_0 \log\left(1 + \gamma_m(t)\right), \tag{2}$$

where B_0 denotes the channel bandwidth.

[1]When the duration of each time slot is small enough, the block fading channel model is a good approximation for the wireless channel in practical systems [34], [35].

[2]It is a broadcast channel in downlink transmission, such that the decoding order of SIC completely depends on the level of transmit power. To enhance the performance of cell-edge users (i.e., with small CPG), it is expected to allocate more power to the users with small CPG. Thus, the optimal decoding order in downlink NOMA netwroks is the ascending order of CPG.

This article has been accepted for publication in a future issue of this journal, but has not been fully edited. Content may change prior to final publication. Citation information: DOI 10.1109/JIOT.2018.2816597, IEEE Internet of Things Journal

Given the control policy $\mathcal{P}(t)$ and $\mathcal{A}(t)$, the total power consumption of the whole network in slot t can be written as

$$\begin{aligned} P^{tot}(t) &= \sum_{m\in\mathcal{U}} p_m(t) + \sum_{m\in\mathcal{U}} a_m(t)\, p_m^c \\ &= \sum_{m\in\mathcal{U}} \left(p_m(t) + a_m(t)\, p_m^c\right). \end{aligned} \tag{3}$$

B. Definitions

Since the concerned network is a dynamic system, we pay attention to its long-term performance (i.e., the long-term average data rate and power consumption) rather than the instantaneous performance. To depict these, we first give the following definition.

Definition 1. *(Time Average Expectation) The time average expectation of a random variable $X(t)$ is defined as*

$$\overline{X} = \lim_{T\to\infty} \frac{1}{T} \sum_{t=1}^{T} \mathbb{E}\left\{X(t)\right\}. \tag{4}$$

According to the above, the long-term average data rate of MD m and the total power consumption of the whole network be respectively expressed as

$$\overline{R}_m\left(\mathcal{P}(t),\, \mathcal{A}(t)\right) = \lim_{T\to\infty} \frac{1}{T} \sum_{t=1}^{T} \mathbb{E}\left\{R_m(t)\right\}. \tag{5}$$

$$\overline{P^{tot}}\left(\mathcal{P}(t),\, \mathcal{A}(t)\right) = \lim_{T\to\infty} \frac{1}{T} \sum_{t=1}^{T} \mathbb{E}\left\{P^{tot}(t)\right\}. \tag{6}$$

Additionally, we also give the definition for the mean rate stable, which will be utilized in the latter parts.

Definition 2. *(Mean Rate Stable) A discrete time process $Y(t)$ is mean rate stable [38] if the following condition is satisfied.*

$$\lim_{t\to\infty} \frac{\mathbb{E}(|Y(t)|)}{t} = 0. \tag{7}$$

C. Problem Formulation

In this paper, we focus on the energy-efficient resource management problem by jointly considering the dynamic user scheduling and power allocation. Particularly, this problem is formulated as the following stochastic optimization problem.

$$\begin{aligned} \min\ & \overline{P^{tot}}\left(\mathcal{P}(t),\, \mathcal{A}(t)\right) \\ \text{s.t. C1}:\ & \overline{R}_m\left(\mathcal{P}(t),\, \mathcal{A}(t)\right) \geq R_m^{\text{req}},\, \forall m \\ \text{C2}:\ & \sum_{m\in\mathcal{U}} p_m(t) \leq P^{\max},\, \forall t \\ \text{C3}:\ & p_m(t) \geq 0,\, \forall m,\, t \\ \text{C4}:\ & a_m(t) = \{0,1\},\, \forall m,\, t \end{aligned} \tag{8}$$

The objective of (8) is to minimize the long-term average power consumption of the whole network including the BS and all MDs. In (8), C1 specifies the long-term average rate requirement of all MDs. C2 limits the maximum instantaneous transmit power of the BS on each channel (also called spectral mask), which is imposed to limits the inter-cell interference. Besides, C3 and C4 indicate the value range of $\mathcal{P}(t)$ and $\mathcal{A}(t)$.

Remark 1. *Problem (8) is very hard to tackle, due to the following reasons. First, it is a long-term optimization problem due to the objective function and constraint C1. Thus, the conventional static optimization techniques are not suitable for it. Furthermore, the binary variable $a_m(t)$ makes (8) a mixed integer programming problem, which is NP-hard in general [39]. Moreover, the existence of intra-cell interference complicates the power allocation, as it results in a non-convex problem. To overcome these difficulties, we exploit the stochastic optimization theory and branch-and-bound method to devise low-complexity and efficient algorithms to solve (8).*

IV. Description of the Proposed Algorithm

In this section, we first transform the primal problem into a tractable one and then propose a dynamic algorith m to solve it based on the stochastic optimization theory, followed by the performance analysis.

A. Problem Transformation

To satisfy the long-term average rate requirement of each MD, we define a set of virtual queues $\mathcal{Q}(t) = \{Q_m(t)\}$, wherein the dynamic of each $Q_m(t)$ is defined as

$$Q_m(t+1) = \left[Q_m(t) + R_m^{\text{req}} - R_m(t)\right]^+, \tag{9}$$

where $[x]^+ = \max\{x, 0\}$. Then, we have the following lemma.

Lemma 1. *If $Q_m(t)$ is mean rate stable, the long-term average rate requirement of MD m is satisfied.*

Proof: According to the dynamic of $Q_m(t)$ (9), we can treat R_m^{req} and $R_m(t)$ as the arrival rate and the departure rate of $Q_m(t)$ in slot t, respectively. If $Q_m(t)$ is mean rate stable, $\mathbb{E}(|Q_m(t)|)$ must be finite (as the Definition 2), that is, the queuing system is stable [40]. From the queuing theory, to maintain the stability of the queuing system, the average arrival rate (i.e., R_m^{req}) must be equal to or smaller than the average departure rate (i.e., $\overline{R}_m$). Therefore, if $Q_m(t)$ is mean rate stable, the average rate requirement of MD m is satisfied. ■

According to Lemma 1, the primal problem (8) can be equivalently recast as

$$\begin{aligned} \min\ & \overline{P^{tot}}\left(\mathcal{P}(t),\, \mathcal{A}(t)\right) \\ \text{s.t. C1}:\ & Q_m(t) \text{ is mean rate stable},\, \forall m \\ \text{C2}:\ & \sum_{m\in\mathcal{U}} p_m(t) \leq P^{\max},\, \forall t \\ \text{C3}:\ & p_m(t) \geq 0,\, \forall m,\, t \\ \text{C4}:\ & a_m(t) = \{0,1\},\, \forall m,\, t. \end{aligned} \tag{10}$$

Compared with the primal problem (8), the above problem (10) is easier to handle, as discussed in the following subsection.

This article has been accepted for publication in a future issue of this journal, but has not been fully edited. Content may change prior to final publication. Citation information: DOI 10.1109/JIOT.2018.2816597, IEEE Internet of Things Journal

B. Description for the Overall Algorithm

In this subsection, we exploit the Lyapunov optimization technique [38] to devise an effective online algorithm to solve (10). First, we define the Lyapunov function as

$$L(\mathcal{Q}(t)) \triangleq \frac{1}{2}\sum_{m\in\mathcal{U}} Q_m(t)^2. \tag{11}$$

Then, the conditional Lyapunov drift in slot t is given by

$$\Delta(\mathcal{Q}(t)) \triangleq \mathbb{E}\left\{L\left(\mathcal{Q}(t+1)\right) - L\left(\mathcal{Q}(t)\right)|\mathcal{Q}(t)\right\}. \tag{12}$$

The objective of (10) is to minimize the total power consumption under the constraints of queue stability. To achieve this goal, we focus on the following drift plus penalty

$$DPP(\mathcal{Q}(t)) = \Delta(\mathcal{Q}(t)) + V\mathbb{E}\left\{P^{tot}(t)|\mathcal{Q}(t)\right\}, \tag{13}$$

where V is a weight.

As shown in (13), minimizing the drift plus penalty $DPP(\mathcal{Q}(t))$ can reduce both the power consumption $P^{tot}(t)$ and the queue backlog $\mathcal{Q}(t)$. Thus, by changing the value of V, we can strike a balance between the queue backlog and the total power consumption. For $DPP(\mathcal{Q}(t))$, we can derive the following conclusion.

Lemma 2. *The upper bound of $DPP(\mathcal{Q}(t))$ is*

$$\begin{aligned} DPP(\mathcal{Q}(t)) \le & \sum_{m\in\mathcal{U}} Q_m(t)\mathbb{E}\left\{R_m^{req} - R_m(t)|\mathcal{Q}(t)\right\} \\ & + V\mathbb{E}\left\{P^{tot}(t)|\mathcal{Q}(t)\right\} + C, \end{aligned} \tag{14}$$

where C is a finite constant.

Proof: For each virtual queue $Q_m(t)$, we can get

$$\begin{aligned} & Q_m(t+1)^2 - Q_m(t)^2 \\ = & \left(\left[Q_m(t) + R_m^{\mathrm{req}} - R_m(t)\right]^+\right)^2 - Q_m(t)^2 \\ \le & \left(Q_m(t) + R_m^{\mathrm{req}} - R_m(t)\right)^2 - Q_m(t)^2 \\ = & \left(R_m^{\mathrm{req}} - R_m(t)\right)^2 + 2Q_m(t)\left(R_m^{\mathrm{req}} - R_m(t)\right). \end{aligned} \tag{15}$$

Since $p_m \le P^{\max}$, $R_m(t)$ must be finite. As such, we can always find a finite constant C that satisfies

$$C \ge \frac{1}{2}\sum_{m\in\mathcal{U}}\left(R_m^{\mathrm{req}} - R_m(t)\right)^2. \tag{16}$$

According to (15) and (16), we can obtain

$$\begin{aligned} & L\left(\mathcal{Q}(t+1)\right) - L\left(\mathcal{Q}(t)\right) \\ = & \frac{1}{2}\sum_{m\in\mathcal{U}} Q_m(t+1)^2 - \frac{1}{2}\sum_{m\in\mathcal{U}} Q_m(t)^2 \\ = & \frac{1}{2}\sum_{m\in\mathcal{U}}\left(Q_m(t+1)^2 - Q_m(t)^2\right) \\ \le & \frac{1}{2}\sum_{m\in\mathcal{U}}\left(2Q_m(t)\left(R_m^{\mathrm{req}} - R_m(t)\right) + \left(R_m^{\mathrm{req}} - R_m(t)\right)^2\right) \\ \le & \sum_{m\in\mathcal{U}} Q_m(t)\left(R_m^{\mathrm{req}} - R_m(t)\right) + C. \end{aligned} \tag{17}$$

Then, adding $VP^{tot}(t)$ to both-hand-sides of the above inequation (17) and taking conditional expectations yield (14). ■

In each slot, minimizing the upper bound of $DPP(\mathcal{Q}(t))$ is helpful for reducing the total power consumption $\overline{P^{tot}}$ and maintaining the stability of each virtual queue $Q_m(t)$, which is the design philosophy of our algorithm. The general algorithm procedure is summarized in Algorithm 1 and detailed in the following. At the beginning of each slot t, the DUSPA observes the instantaneous network state (virtual queues[3] $\mathcal{Q}(t) = \{Q_m(t)\}$and channel conditions $\mathcal{G}(t) = \{g_m(t)\}$). Then, the DUSPA obtains the control policies $\mathcal{A}^*(t) = \{a_m(t)\}$ and $\mathcal{P}^*(t) = \{p_m(t)\}$ in slot t by solving the optimization problem (18). With the execution results, the DUSPA finally updates each virtual queue $Q_m(t+1)$. The aforementioned operations are repeated and the network eventually reaches a steady state, where the average total power consumption is bounded and the rate requirements of all MDs are satisfied.

Algorithm 1 Dynamic user scheduling and power allocation algorithm (DUSPA)

1: At the beginning of each slot, observe the virtual queues $\mathcal{Q}(t)=\{Q_m(t)\}$ and channel conditions $\mathcal{G}(t)=\{g_m(t)\}$.

2: Determine the control policies $\mathcal{A}^*(t) = \{a_m(t)\}$ and $\mathcal{P}^*(t) = \{p_m(t)\}$ by solving the following problem.

$$\begin{aligned} \min_{\mathcal{A}(t),\mathcal{P}(t)} \; & VP^{tot}(t) - \sum_{m\in\mathcal{U}} Q_m(t)R_m(t) \\ \text{s.t. C1}: \; & \sum_{m\in\mathcal{U}} p_m(t) \le P^{max} \\ \text{C2}: \; & p_m(t) \ge 0, \forall m \\ \text{C3}: \; & a_m(t) = \{0,1\}, \forall m. \end{aligned} \tag{18}$$

3: Update each virtual queues $Q_m(t+1)$ according to the control policies $\{\mathcal{A}^*(t), \mathcal{P}^*(t)\}$ and equation (18).

Remark 2. *The DUSPA is an online algorithm that can make decisions but without requiring any statistical knowledge of the channel conditions. This is a good feature for the application of the proposed algorithm into a practical system. It is noted that even by this simple way, the DUSPA can still achieve good performance in power consumption and satisfy the long-term rate requirements of all MDs, discussed in the following subsection.*

C. Performance Analysis

Lemma 3. *The proposed DUSPA can satisfy the long-term rate requirements of all MDs.*

Proof: It has been proofed in [38], [41] that if (10) is feasible, then for any $\delta > 0$, there must exist a stationary randomized policy[4] that satisfies

$$\mathbb{E}\left\{\widehat{P^{tot}}(t)|\mathcal{Q}(t)\right\} = \mathbb{E}\left\{\widehat{P^{tot}}(t)\right\} \le P^{\min} + \delta, \tag{19}$$

$$\mathbb{E}\left\{R_m^{req} - \widehat{R_m}(t)|\mathcal{Q}(t)\right\} = \mathbb{E}\left\{R_m^{req} - \widehat{R_m}(t)\right\} \le \delta, \forall m \tag{20}$$

[3]Without loss of generality, each $Q_m(t)$ in the first slot is set to zero.

[4]The stationary randomized policy is independent on the queue backlog information, which makes decisions only according to the instantaneous random events in each slot [38], [41].

This article has been accepted for publication in a future issue of this journal, but has not been fully edited. Content may change prior to final publication. Citation information: DOI 10.1109/JIOT.2018.2816597, IEEE Internet of Things Journal

where $\widehat{P^{tot}}(t)$ and $\widehat{R_m}(t)$ are the resulting values derived by the stationary randomized policy, δ is an arbitrarily small positive number, and $P^{\min}$ is the minimum value of the objective function in (10).

As previously mentioned, the DUSPA can minimize the upper bound of $DPP(\mathcal{Q}(t))$, such that

$$\begin{aligned}&\Delta(\mathcal{Q}(t))+V\mathbb{E}\left\{P^{tot}(t)|\mathcal{Q}(t)\right\}\\ \le&\sum_{m\in\mathcal{U}}Q_m(t)\mathbb{E}\left\{R_m^{req}-\widetilde{R_m}(t)|\mathcal{Q}(t)\right\}+V\mathbb{E}\left\{\widetilde{P^{tot}}(t)|\mathcal{Q}(t)\right\}+C\\ \le&\sum_{m\in\mathcal{U}}Q_m(t)\mathbb{E}\left\{R_m^{req}-\widehat{R_m}(t)|\mathcal{Q}(t)\right\}+V\mathbb{E}\left\{\widehat{P^{tot}}(t)|\mathcal{Q}(t)\right\}+C,\end{aligned} \tag{21}$$

where $\widetilde{P^{tot}}(t)$ and $\widetilde{R_m}(t)$ are the resulting values derived by the DUSPA.

Plugging (19) and (20) into (21), we can obtain

$$\begin{aligned}&\Delta(\mathcal{Q}(t))+V\mathbb{E}\left\{P^{tot}(t)|\mathcal{Q}(t)\right\}\\ \le&C+VP^{\min}-\delta\sum_{m\in\mathcal{U}}Q_m(t)\\ \le&C+VP^{\min}.\end{aligned} \tag{22}$$

Taking iterated expectation in the above inequality over $t\in\{1,2,\cdots,T\}$ and using telescoping sums yield

$$\begin{aligned}&\mathbb{E}\left\{L(\mathcal{Q}(T))\right\}-\mathbb{E}\left\{L(\mathcal{Q}(1))\right\}+V\sum_{t=1}^{T}\mathbb{E}\left\{P^{tot}(t)\right\}\\ \le&T\left(C+VP^{\min}\right).\end{aligned} \tag{23}$$

Let $\mathbb{E}\left\{P^{tot}(t)\right\}=0$ and rearranging (23), we can get

$$\mathbb{E}\left\{L(\mathcal{Q}(T))\right\}\le T\left(C+VP^{\min}\right)+\mathbb{E}\left\{L(\mathcal{Q}(1))\right\}. \tag{24}$$

According to the definition of $L(\mathcal{Q}(T))$, it can be obtained

$$\frac{1}{2}\sum_{m\in\mathcal{U}}\mathbb{E}\left\{Q_m(t)^2\right\}\le T\left(C+VP^{\min}\right)+\mathbb{E}\left\{L(\mathcal{Q}(1))\right\}. \tag{25}$$

Due to the fact of $\mathbb{E}\left\{|Q_m(t)|\right\}^2\le\mathbb{E}\left\{Q_m(t)^2\right\}$, we can get

$$\mathbb{E}\left\{|Q_m(t)|\right\}\le\sqrt{2T\left(C+VP^{\min}\right)+2\mathbb{E}\left\{L(\mathcal{Q}(1))\right\}}. \tag{26}$$

Since the right hand side of (26) is a finite value, it can be easily proved

$$\lim_{t\to\infty}\frac{\mathbb{E}\left\{|Q_m(t)|\right\}}{t}=0. \tag{27}$$

Hence, all virtual queues $\mathcal{Q}(t)$ are mean rate stable. Recall to Lemma 1, we can know that the rate requirements of all users can be satisfied by the proposed DUSPA. ■

V. Algorithm Design for the Resource Management Problem in Each Slot

In this section, we employ the branch-and-bound method to design an efficient algorithm to solve the instantaneous resource management problem embedded in the DUSPA.

A. Problem Transformation

As shown in Algorithm 1, a key step of the DUSPA is to acquire the optimal solution of (18), otherwise the constraint C1 in (10) cannot be strictly satisfied. However, (18) is a mixed-integer and non-convex programming, which is difficult to tackle. To deal with this difficulty, we first transform (18) into another form without changing its nature. In particular, we define $\mathcal{R}(t)=\{r_m(t)\}$ where $r_m(t)$ is defined as

$$r_m(t)=B_0\log\left(1+\gamma_m(t)\right). \tag{28}$$

Through variable substitution, we can reformulate (18) as given in the following Lemma.

Lemma 4. *Problem (18) can be equivalently reformulated as*

$$\begin{aligned}\min_{\mathcal{R}(t),\mathcal{A}(t)}\ &V\sum_{m\in\mathcal{U}}W_m(t)2^{\sum_{i=1}^{m}\frac{r_m(t)}{B_0}}+V\sum_{m\in\mathcal{U}}a_m(t)p_m^c\\ &-\sum_{m\in\mathcal{U}}Q_m(t)r_m(t)\\ \text{s.t. C1}:\ &\sum_{m\in\mathcal{U}}W_m(t)2^{\sum_{i=1}^{m}\frac{r_m(t)}{B_0}}-\frac{\sigma^2}{g_0(t)}\le P^{\max}\\ \text{C2}:\ &0\le r_m(t)\le a_m(t)r_m^{\max}(t),\ \forall m\\ \text{C3}:\ &a_m(t)=\{0,1\},\ \forall m,\end{aligned} \tag{29}$$

where $W_m(t)=\frac{\sigma^2}{g_m(t)}-\frac{\sigma^2}{g_{m+1}(t)}$, $g_{M+1}(t)=+\infty$, *and* $r_m^{\max}(t)=B_0\log\left(1+\frac{P^{\max}(t)g_m(t)}{\sigma^2}\right)$.

Proof: According to (1) and (28), we can obtain

$$p_m(t)=\left(2^{\frac{r_m(t)}{B_0}}-1\right)\left(\sum_{i\in\mathcal{U},i>m}p_i(t)+\frac{\sigma^2}{g_m(t)}\right). \tag{30}$$

Rearranging the above formula, we have

$$\sum_{i=m}^{M}p_i(t)=2^{\frac{r_m(t)}{B_0}}\sum_{i=m+1}^{M}p_i(t)+\frac{\sigma^2}{g_m(t)}\left(2^{\frac{r_m(t)}{B_0}}-1\right). \tag{31}$$

Adopting the recursive method for (31), we can acquire the total transmit power of the BS as

$$\begin{aligned}\sum_{m\in\mathcal{U}}p_m(t)=&\sum_{m=1}^{M-1}\left(\frac{\sigma^2}{g_m(t)}-\frac{\sigma^2}{g_{m+1}(t)}\right)2^{\sum_{i=1}^{m}\frac{r_m(t)}{B_0}}\\ &+\frac{\sigma^2}{g_M(t)}2^{\sum_{i=1}^{M}\frac{r_m(t)}{B_0}}-\frac{\sigma^2}{g_0(t)}\\ =&\sum_{m\in\mathcal{U}}W_m(t)2^{\sum_{i=1}^{m}\frac{r_m(t)}{B_0}}-\frac{\sigma^2}{g_0(t)}.\end{aligned} \tag{32}$$

Besides, it can be easily proofed

$$\begin{aligned}r_m(t)=&B_0\log\left(1+\frac{p_m(t)g_m(t)}{\sum_{i\in\mathcal{U},i>m}p_i(t)g_m(t)+\sigma^2}\right)\\ \le&B_0\log\left(1+\frac{P^{\max}(t)g_m(t)}{\sigma^2}\right).\end{aligned} \tag{33}$$

This article has been accepted for publication in a future issue of this journal, but has not been fully edited. Content may change prior to final publication. Citation information: DOI 10.1109/JIOT.2018.2816597, IEEE Internet of Things Journal

Replacing $\mathcal{R}(t)$ by $\mathcal{P}(t)$ and removing $\frac{\sigma^2}{g_0(t)}$ from the objective function, we can transform (18) into the following form.

$$\begin{aligned}\min_{\mathcal{R}(t),\mathcal{A}(t)}\ & V\sum_{m\in\mathcal{U}} W_m(t)2^{\sum_{i=1}^{m}\frac{r_m(t)}{B_0}} + V\sum_{m\in\mathcal{U}} a_m(t)\,p_m^c \\ & -\sum_{m\in\mathcal{U}} Q_m(t)a_m(t)\,r_m(t) \\ \text{s.t. C1}:\ & \sum_{m\in\mathcal{U}} W_m(t)2^{\sum_{i=1}^{m}\frac{r_m(t)}{B_0}} - \frac{\sigma^2}{g_0(t)} \le P^{\max} \\ \text{C2}:\ & 0\le r_m(t)\le r_m^{\max}(t),\ \forall m \\ \text{C3}:\ & a_m(t)=\{0,1\},\ \forall m. \end{aligned} \tag{34}$$

Considering the feature that when $a_m(t)=0$, $R_m(t)=0$ and when $a_m(t)=1$, $R_m(t)=r_m(t)$, we can equivalently recast (34) as (29), such that the product term $a_m(t)\,r_m(t)$ is eliminated from the objective function.

To this end, we have proofed Lemma 4. ∎

For the optimization problem (29), we have the following Lemma.

Lemma 5. *If each $a_m(t)$ is relaxed to [0, 1], i.e., $a_m(t)\in[0,1],\forall m$, then (29) becomes a convex optimization problem.*

Proof: Because of $g_m(t)\le g_{m+1}(t),\forall m$, $W_m(t)=\frac{\sigma^2}{g_m(t)}-\frac{\sigma^2}{g_{m+1}(t)}$ is thus non-negative for each m. If $a_m(t),\forall m$ is relaxed to [0, 1], the objective function in (29) becomes convex as it is the sum of some convex and linear functions. Furthermore, all constraints in (29) are either convex or linear. Therefore, the relaxed problem of (29) (*i.e.,* $a_m(t)\in[0,1],\forall m$) is a convex optimization problem. ∎

Based on Lemma 5, we will adopt the branch-and-bound method [42], [43] to design a low-complexity algorithm to acquire the optimal solutions of (29). The designed algorithm consists of three main procedures, i.e., branching, bounding, and pruning. In what follows, we will introduce these procedures in detail.

B. Branching

The branching procedure is to create smaller subproblems by constantly trying the scheduling schemes for each MD. In our concerned problem, each MD has two states, i.e., scheduled state $a_m(t)=1$ or unscheduled state $a_m(t)=0$, thereby the branching procedure can be described by a binary tree as shown in Fig. 2. The whole binary tree is denoted by $\mathcal{T}$, wherein $\mathcal{T}_k$ represents the set of branches in the k-th layer. As depicted in Fig. 2, $\mathcal{T}_k$ contains at most 2^k branches, each of which records a user scheduling scheme for the k tested users. Particularly, let $\mathcal{S}_j$ $(j=1,2,\cdots,|\mathcal{T}_k|)$ denote the user scheduling scheme corresponding to the j-th branch in $\mathcal{T}_k$. For instance, in $\mathcal{T}_2$ of Fig. 2, $\mathcal{S}_1$ represents the user scheduling scheme $\{a_{k_1}(t)=0, a_{k_2}(t)=0\}$ and $\mathcal{S}_4$ represents $\{a_{k_1}(t)=1, a_{k_2}(t)=1\}$.

For each branch $\mathcal{S}_j$, we should solve the following convex problem, the optimal value of which is denoted by $f(\mathcal{S}_j)$.

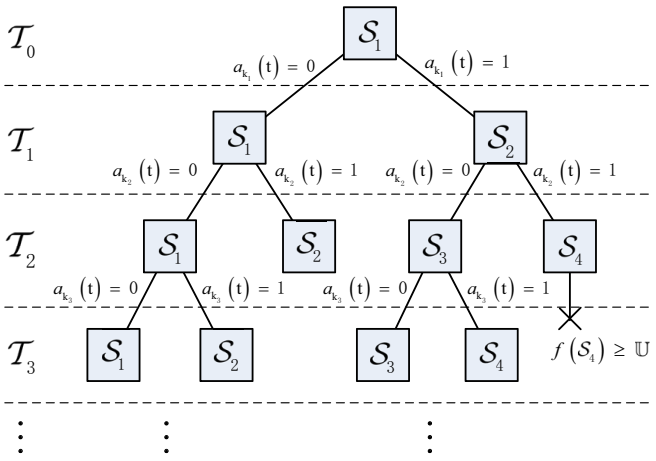

Figure 2. Illustration for the branch-and-bound procedure.

$$\begin{aligned}\min_{\mathcal{R}(t),\mathcal{A}(t)}\ & V\sum_{m\in\mathcal{U}} W_m(t)2^{\sum_{i=1}^{m}\frac{r_m(t)}{B_0}} + V\sum_{m\in\mathcal{U}} a_m(t)\,p_m^c \\ & -\sum_{m\in\mathcal{U}} Q_m(t)r_m(t) \\ \text{s.t. C1}:\ & \sum_{m\in\mathcal{U}} W_m(t)2^{\sum_{i=1}^{m}\frac{r_m(t)}{B_0}} - \frac{\sigma^2}{g_0(t)} \le P^{\max} \\ \text{C2}:\ & 0\le r_m(t)\le a_m(t)\,r_m^{\max}(t),\ \forall m \\ \text{C3}:\ & 0\le a_m(t)\le 1,\ \forall m\notin\mathcal{S}_j \\ \text{C4}:\ & a_m(t)\ \text{is the given value},\ \forall m\in\mathcal{S}_j. \end{aligned} \tag{35}$$

In the branching procedure, it is of great importance to decide which user should be selected for testing. This is because it directly affects the updating rate of $\mathbb{U}$, the criterion of the pruning operation, and thus affects the computational complexity of the whole algorithm. To find a feasible solution of (29) as soon as possible, we primarily choose the MD who has the most uncertainty in the scheduling state. Specifically, the user selection rule in the k-th layer is

$$m_k=\arg\max_{\mathrm{m}\in\mathcal{U}}\ \sum_{j=1}^{|\mathcal{T}_{k-1}|}|a_m^j(t)-0.5|, \tag{36}$$

where $a_m^i(t)$ represents the scheduling solution of MD m obtained by solving the relaxed problem (35) with the j-th branch $\mathcal{S}_j$ in layer $\mathcal{T}_{k-1}$. By this rule, the number of non-binary solutions of $\{a_m(t)\}$ can be quickly reduced, and thus accelerates the speed of finding the optimal solution.

C. Bounding

In our designed algorithm, an upper bound of (29) is preserved and updated constantly, which is denoted by $\mathbb{U}$. The main role of $\mathbb{U}$ is utilized to prune the branches without the optimal solutions, which will be discussed in the following subsection. Specifically, $\mathbb{U}$ is set to the objective function value of (29) derived by its feasible solutions. During the execution of the algorithm, if a better feasible solution is obtained (that is, $f(\mathcal{S}_j)<\mathbb{U}$ and all $a_m(t),\forall m$ are binary), $\mathbb{U}$ will be

This article has been accepted for publication in a future issue of this journal, but has not been fully edited. Content may change prior to final publication. Citation information: DOI 10.1109/JIOT.2018.2816597, IEEE Internet of Things Journal

updated as $f(\mathcal{S}_j)$, otherwise $\mathbb{U}$ remains unchanged. As such, $\mathbb{U}$ is reduced gradually and equal to the optimal value of (29) at the end of the algorithm.

D. Pruning

The pruning procedure is to prune the branches that do not contain the optimal solutions. By this way, the searching space can be greatly reduced, and hence improving the efficiency of the proposed algorithm. As illustrated in Fig. 2, two branches are pruned in $\mathcal{T}_3$, such that the searching space is reduced by half. In our designed algorithm, there are two cases that a branch can be pruned. One case is that the optimal value of the relaxed problem (35) is still smaller than the upper bound $\mathbb{U}$. In this case, the objective function value of all feasible solutions must be smaller than $\mathbb{U}$ as well, that is, the optimal solution cannot exist in this branch, an hence this branch can be pruned with no need for further searching. Another case is that a better feasible solution of (29) is obtained. In this case, all $a_m(t), \forall m$ are binary, thereby it is also no need to test the user scheduling schemes for the remainder MDs.

E. Description of the Proposed Algorithm

The proposed algorithm is summarized in Algorithm 2, referred to as BBA. In the initialization phase, we set $\mathbb{U} = +\infty$, such that $\mathbb{U}$ can be updated by any feasible solutions of (29). At the beginning of the algorithm, we first solve the relaxed problem (35) with $\mathcal{S}_j = \emptyset$. If all $a_m(t)$ are binary, that is the optimal solution is obtained, the algorithm can be terminated directly. Otherwise, the aforementioned branching, bounding, and pruning operations will be repeated by the BBA until all control policies $\{\mathcal{P}(t), \mathcal{A}(t)\}$ are tested or removed. By this way, the optimal control policy $\{\mathcal{P}^*(t), \mathcal{A}^*(t)\}$ can be obtained at the termination of the BBA.

Remark 3. *From Algorithm 2, we can find that every user scheduling scheme is tested or pruned at the end of the algorithm. Thus, the BBA can obtain the same solution with the exhaustive search method, but the computational complexity is greatly reduced through the well-designed branching, bounding, and pruning operations.*

Algorithm 2 Branch-and-bound based algorithm (BBA)

1: **Initialization:**
- Set $\mathbb{U} = +\infty$ and $\mathcal{T}_0 = \{\mathcal{S}_1 = \emptyset\}$.
- Set $\{\mathcal{P}^*(t) = \emptyset, \mathcal{A}^*(t) = \emptyset\}$.

2: Solve the relaxed problem (35) with $\mathcal{S}_j = \emptyset$. If all $a_m(t)$ are binary, update $\{\mathcal{P}^*(t), \mathcal{A}^*(t)\}$ and go to step 12.
3: **for** $k = 1 : M$ **do**
4: **for** $j = 1 : |\mathcal{T}_{k-1}|$ **do**
5: Select the branch $\mathcal{S}_j$ from $\mathcal{T}_{k-1}$.
6: Choose MD m_k according to (36).
7: Split $\mathcal{S}_j$ into two branches $\mathcal{S}_j^1$ and $\mathcal{S}_j^2$, where $\mathcal{S}_j^1 = \mathcal{S}_j \cup \{a_{m_k}(t) = 0\}$ and $\mathcal{S}_j^2 = \mathcal{S}_j \cup \{a_{m_k}(t) = 1\}$;
8: Solve the relaxed problem (35) with $\mathcal{S}_j = \mathcal{S}_j^1$ and get the objective function value $f(\mathcal{S}_j^1)$. If $f(\mathcal{S}_j^1) < \mathbb{U}$ and all $a_m(t)$ are binary, update $\mathbb{U} = f(\mathcal{S}_j^1)$ and $\{\mathcal{P}^*(t), \mathcal{A}^*(t)\}$. If $f(\mathcal{S}_j^1) < \mathbb{U}$ and but not all $a_m(t)$ are binary, add $\mathcal{S}_j^1$ into $\mathcal{T}_k$.
9: Solve the relaxed problem (35) with $\mathcal{S}_j = \mathcal{S}_j^2$ and get the objective function value $f(\mathcal{S}_j^2)$. If $f(\mathcal{S}_j^2) < \mathbb{U}$ and all $a_m(t)$ are binary, udpate $\mathbb{U} = f(\mathcal{S}_j^2)$ and $\{\mathcal{P}^*(t), \mathcal{A}^*(t)\}$. If $f(\mathcal{S}_j^2) < \mathbb{U}$ and but not all $a_m(t)$ are binary, add $\mathcal{S}_j^2$ into $\mathcal{T}_k$.
10: **end for**
11: **end for**
12: **Output:** The optimal control policy $\{\mathcal{P}^*(t), \mathcal{A}^*(t)\}$.

VI. Simulation Results

In this section, we present simulation results to evaluate the performance of the proposed algorithm (DUSPA). The common simulation parameters are listed in Tab. I. In the simulations, the mobile devices are uniformly distributed in the coverage area of the BS. Firstly, we investigate the convergence of the DUSPA as well as the effect of the control factor V on the network performance. Then, we compare the DUSPA with another two schemes (namely OFDMA-RR and NOMA-PA) to demonstrate the performance gain brought by jointly optimizing user scheduling and power allocation. More detailedly, the OFDMA-RR adopts the traditional orthogonal multiple access technique OFDMA with round-robin user scheduling policy so as to accommodate all MDs. As such, each MD can only be served in one M-th of the time. To satisfy the long-term rate requirement of each MD, the instantaneous rate constraint for the scheduled MDs is promoted to $M \times R_m^{\text{req}}$. Additionally, for the NOMA-PA, all MDs are scheduled in each slot with optimized power allocation aiming to minimize the transmit power of the BS [20].

Table I
Simulation parameters

Cell radius	1000 m
Path loss	128.1+37.6$\log_{10}(d[km])$
Shadowing	Log normal as $\mathcal{N}(0, 8^2)$
Fading	Rayleigh fading with 1 variance
Noise Power, σ^2	1.8×10^{-13} Watt
Spectral mask, $P^{\max}$	4 Watt
Circuit power consumption, p_m^c	0.2 Watt
Channel bandwidth, B_0	180 KHz
Simulation times	5000

A. Convergence Performance

Fig. 3 shows the convergence of the average total power consumption and the average virtual queue backlog versus the number of iterations. From this figure, we can find that given the rate requirement, our designed algorithm can converge to a balance point with the increment of the number of iterations. This is because at the beginning of the algorithm, the virtual queue backlog of each MD is zero. According to the drift plus penalty equation (13), we can know that the DUSPA is more inclined to reduce the total power consumption in the early phase. As a consequence, the achievable data rate of each MD is usually smaller than its demand, which results in the rapid increment of the the virtual queue backlog as

This article has been accepted for publication in a future issue of this journal, but has not been fully edited. Content may change prior to final publication. Citation information: DOI 10.1109/JIOT.2018.2816597, IEEE Internet of Things Journal

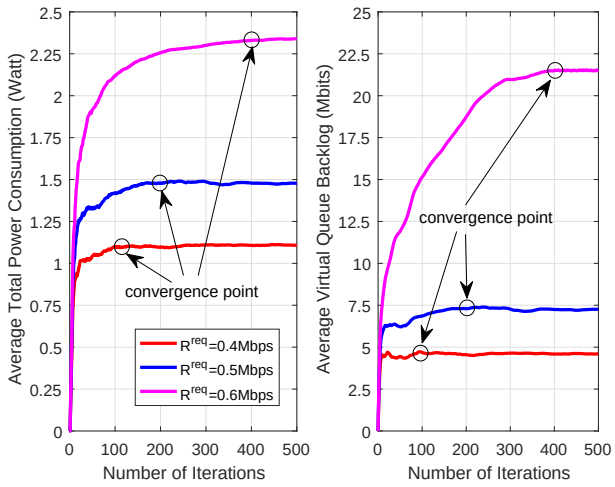

Figure 3. Convergence of the average total power consumption and the average vitrual queue backlog ($M = 6$, $V = 0.5$, $R_m^{\mathrm{req}} = R^{\mathrm{req}}, \forall m$, one channel).

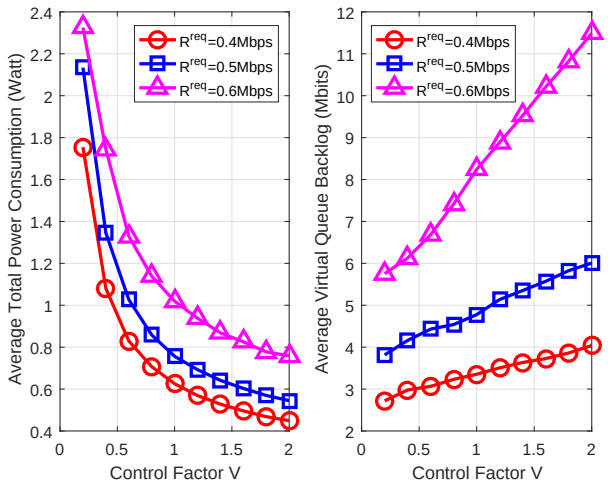

Figure 5. Effect of the control factor V on the total power consumption and the queue backlog ($M = 6$, $V = 0.5$, $R_m^{\mathrm{req}} = R^{\mathrm{req}}, \forall m$, one channel).

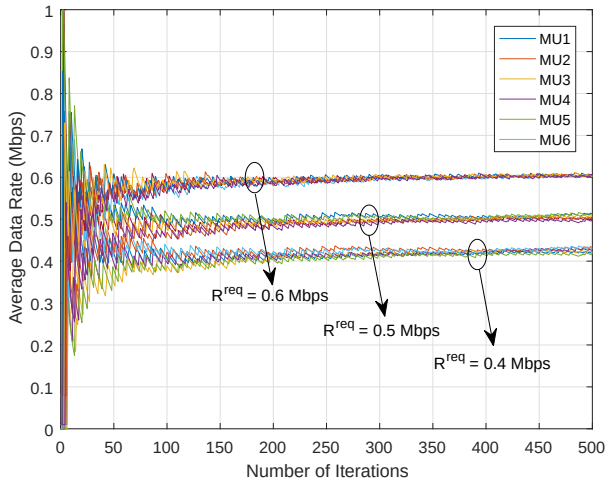

Figure 4. Convergence of the average achievable data rate ($M = 6, V = 0.5$, $R_m^{\mathrm{req}} = R^{\mathrm{req}}, \forall m$, one channel).

depicted in Fig. 3. To restrain the sustained increment of the queue backlog, more power will be consumed by the DUSPA to enhance the data rate of each MD, and thus the total power consumption will increase as well. Fig. 3 shows that the total power consumption and the virtual queue backlog increase continually until a balance between them is striked. Furthermore, since large rate requirement leads to large queue backlog, more power and convergence time will be consumed accordingly.

Fig. 4 plots the convergence of the average data rate of each MD versus the number of iterations. It can be observed from this figure that the average data rate of each MD is dynamically changing at the early stage and then levels off with the increment of iterations. The reason is that MDs are dynamically scheduled by the DUSPA in each slot. If their rate requirements are not met, large data rate will be achieved for the scheduled MDs, while none for the unscheduled MDs. As such, the average data rate of each MD fluctuates obviously at the early stage. However, as the algorithm proceeds, the gap between the rate requirement and acquisition narrows gradually, and hence the average data rate levels off when the number of iterations is large. This simulation result confirms that our algorithm can satisfy the long-term rate requirements of all MDs (i.e., Lemma 3).

Fig. 5 depicts the effect of the control factor V on the total power consumption and the queue backlog. As can be seen, the total power consumption decays with V exponentially, while the queue backlog increases with V linearly. Along with the increment of V, the total power consumption reaches a certain value asymptotically, but the queue backlog becomes infinite. Since Little's Theorem [31] indicates that average delay is proportional to average queue length for a stable system, the delay in NOMA networks will become intolerant for users when V is very large. Therefore, it is irrational to set V too large even for minimizing the total power consumption. In a practical system, V should be selected with full consideration of the tradeoff between the power consumption and the delay.

B. Performance Comparison

Fig. 6 illustrates the average total power consumption of different algorithms versus the number of MDs[5]. The simulation results indicate that our algorithm can greatly reduce the power consumption compared with the other two schemes. With respect to the OFDMA-RR, our algorithm can fully exploit user diversities in the power domain, thereby it can use less power to serve more users in one slot. However, the OFDMA-RR can only serve one user on each time-frequency resource block. Thus, to satisfy the long-term rate requirements of all MDs, the OFDMA-RR should utilize very large transmit power to meet the amplified instantaneous rate

[5]It is assumed that the MDs are uniformly distributed on each channel. We do not formulate the channel assigenment into the considered problem, mainly because the channel assignemt is not the main concern of this paper and taking it into account will complicates the algorithm design.

This article has been accepted for publication in a future issue of this journal, but has not been fully edited. Content may change prior to final publication. Citation information: DOI 10.1109/JIOT.2018.2816597, IEEE Internet of Things Journal

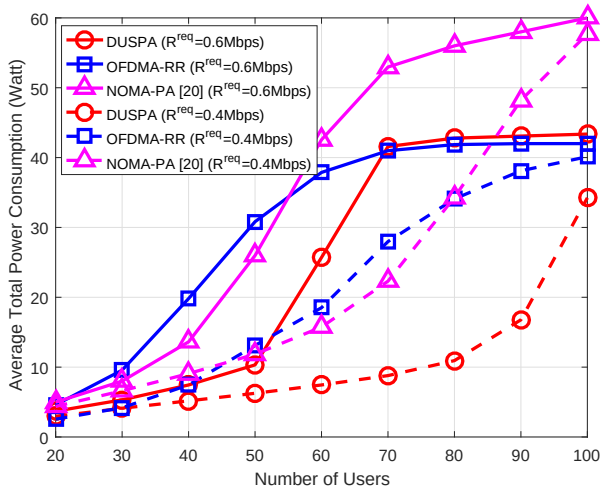

Figure 6. Average total power consumption versus the number of MDs ($V = 1$, $R_m^{\text{req}} = R^{\text{req}}, \forall m$, 10 channels).

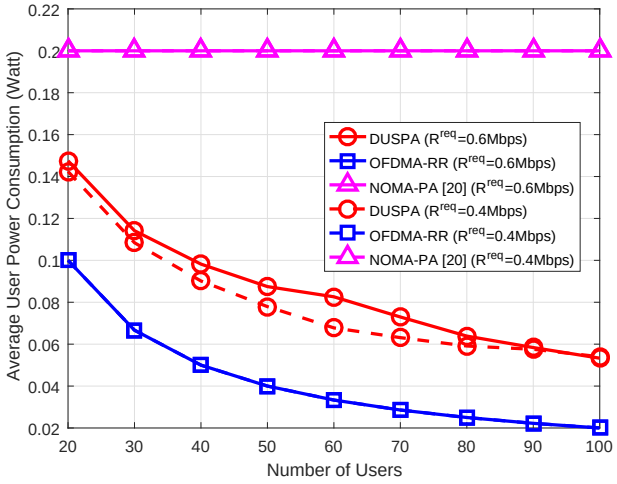

Figure 8. Average user power consumption versus the number of MDs ($V = 1$, $R_m^{\text{req}} = R^{\text{req}}, \forall m$, 10 channels).

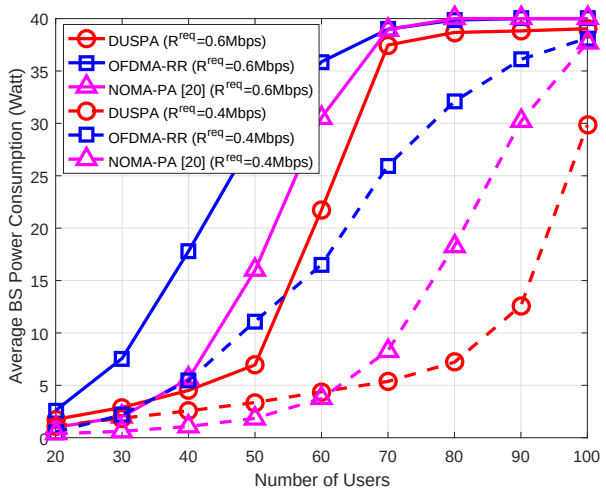

Figure 7. Average BS power consumption versus the number of MDs ($V = 1$, $R_m^{\text{req}} = R^{\text{req}}, \forall m$, 10 channels).

requirement (i.e., $M \times R_m^{\text{req}}$). In comparison with the NOMA-PA, our algorithm can choose appropriate users to be served in each slot via dynamic user scheduling. By this way, the near-far effect of users can be fully exploited, and meanwhile the intra-cell interference is controlled at a tolerable level. In contrast, serving all users at the same time not only makes the near-far effect non-obvious but also results in large intra-cell interference and hence large power consumption especially for large number of users. This also accounts for why the NOMA-PA consumes more power than the OFDMA-RR when the number of users is large.

Fig. 7 illustrates the effect of user number on the BS power consumption. It can be observed that the trend of the BS power consumption versus the number of MDs is almost identical with that given in Fig. 6. This is mainly because the total power consumption of the whole network is dominated by the transmit power of the BS. From this figure, we can find that the NOMA-PA can save more power than the proposed algorithm when the number of users is small. The reason is that the goal of the NOMA-PA is to minimize the transmit power of the BS, while the DUSPA aims to reduce the power consumption of the whole network (i.e., the BS and all MDs). With small number of users, the NOMA-PA can use less transmit power to serve all users, but the condition will reverse with the increment of users. Besides, this figure shows that in the scenario with massive connections, NOMA outperforms OFDMA in terms of the BS power consumption and the transmit power of the BS can be further reduced by appropriate user scheduling. Furthermore, from this figure, we can find that when the number of MDs is larger than 70 for R^{req}=0.6 Mbps, the consumed power of the BS under all algorithms has reached the upper bound of the transmit power. At this point, the network cannot strictly satisfy the rate requirements of all MDs. Due to this reason, our algorithm has no advantages in respect of the power consumption (as shown in Fig. 6 and Fig. 7), however we will demonstrate in the following (as shown in Fig. 10) that even in this case, our algorithm can still provide better service compared with the other two schemes.

Fig. 8 shows the average user power consumption versus the number of users. It is noted that the power consumption of a user depends on the frequency of the user scheduled in the time domain. More frequency the user scheduled, more power will be consumed accordingly. From this figure, we can find that the power consumed by each user under the NOMA-PA is always 0.2 Watt. This is because in the NOMA-PA, all users must keep awake for data reception, just as depicted in Fig. 9 which shows the average number of users scheduled in each slot. The NOMA-PA schedules users without regard to their achievable data rate, thus this scheme is inefficiency. On the other hand, users are scheduled in a round-robin manner under the OFDMA-RR. As shown in Fig. 9, the number of users scheduled by the OFDMA-RR is always equal to the number of channels, thereby the normalized serving time acquired by each user (or average user power consumption) decreases with the number of users by the law of 1/M. Although the

This article has been accepted for publication in a future issue of this journal, but has not been fully edited. Content may change prior to final publication. Citation information: DOI 10.1109/JIOT.2018.2816597, IEEE Internet of Things Journal

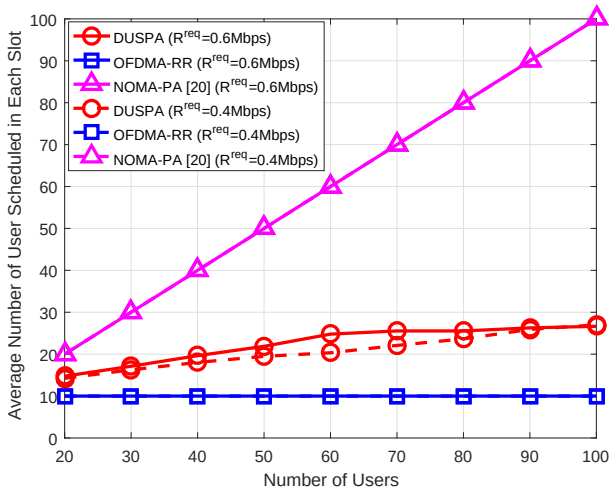

Figure 9. Average number of users scheduled in each slot versus the number of MDs ($V = 1$, $R_m^{\mathrm{req}} = R^{\mathrm{req}}, \forall m$, 10 channels).

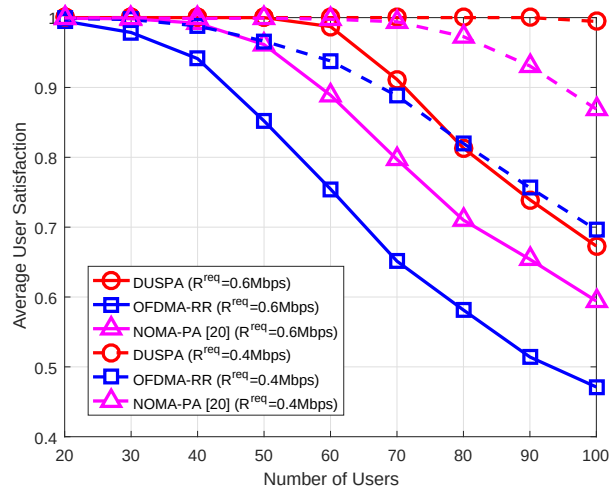

Figure 10. User satisfaction versus the number of MDs ($V = 1$, $R_m^{\mathrm{req}} = R^{\mathrm{req}}, \forall m$, 10 channels).

OFDMA-RR produces the lowest user power consumption, it also generates the largest BS power consumption shown in Fig. 7. In conclusion, the NOMA-PA and the OFDMA-RR are two extremes in user scheduling, both of which cannot achieve the optimal network performance. By contrast, our algorithm can make a tradeoff between them and thus exhibits good performance in power consumption at both the BS side and the user side. Besides, it can be observed from Fig. 9 that the optimal number of users scheduled on each channel is 2-3, which is a valuable conclusion for the design of practical NOMA networks.

Fig. 10 presents the user satisfaction of different algorithms versus the number of MDs, where the user satisfaction is defined as $\min\left\{1, \overline{R}_m / R_m^{\mathrm{req}}\right\}$. From this figure, we can observe that with $R_m^{\mathrm{req}} = 0.4\mathrm{Mbps}$, our algorithm can satisfy all users' rate requirements, while the other two schemes cannot guarantee this demand. Besides, we can find that NOMA outperforms OFDMA in terms of user satisfaction, as NOMA can serve more users in each slot. This result indicates that NOMA is more suitable for the scenario with massive connections. For $R_m^{\mathrm{req}} = 0.6\,\mathrm{Mbps}$, all schemes cannot guarantee the long-term rate requirements of all users especially when the number of users exceeds 60. However, by contrast, our algorithm can still achieve a good performance in comparison with the other two schemes. In this case, our algorithm can accommodate at most 60 users under the power constraint of the BS. When the number of users exceeds 60, the maximum power constraint $P^{\max}$ is reached, and thus our algorithm cannot satisfy the rate requirements of all users. The simulation results verify that our algorithm can save more power in low traffic condition and provide better user satisfaction in high traffic condition.

VII. Conclusion

In this paper, we have investigated the total power consumption minimization problem for NOMA downlink networks by jointly considering user scheduling and power allocation. Particularly, this problem has been formulated as a stochastic optimization problem. To tackle this intractable problem, we have exploited the Lyapunov optimization technique and the branch-and-bound method to devise a low-complexity and easy-implemented online algorithm. Only according to the instantaneous system state, the proposed algorithm can make real-time decisions to guarantee the long-term network performance. Finally, simulation results have verified the effectiveness of the proposed algorithm by comparing it with other schemes.

References

[1] IMT-2020 5G Promotion Group, "5G vision and requirements," White paper, May 2014.

[2] L. Sun and Q. Du, "Physical layer security with its applications in 5G networks: A review," *China Communications*, vol. 14, no. 12, pp. 1–14, Dec. 2017.

[3] IMT-2020 5G Promotion Group, "5G wireless technology architecture," White paper, May 2015.

[4] 3GPP TD RP-150496, "Study on downlink multiuser superposition transmission."

[5] L. Dai, B. Wang, Y. Yuan, S. Han, C. l. I, and Z. Wang, "Non-orthogonal multiple access for 5G: solutions, challenges, opportunities, and future research trends," *IEEE Commun. Mag.*, vol. 53, no. 9, pp. 74–81, Sep. 2015.

[6] Y. Saito, Y. Kishiyama, A. Benjebbour, T. Nakamura, A. Li, and K. Higuchi, "Non-orthogonal multiple access (NOMA) for cellular future radio access," in *Proc. IEEE VTC'13-spring, Dresden, Germany*, Jun. 2013, pp. 1–5.

[7] Z. Ding, Y. Liu, J. Choi, Q. Sun, M. Elkashlan, C. L. I, and H. V. Poor, "Application of non-orthogonal multiple access in LTE and 5G networks," *IEEE Commun. Mag.*, vol. 55, no. 2, pp. 185–191, Feb. 2017.

[8] J. Zhu, Y. Song, D. Jiang, and H. Song, "A new deep-q-learning-based transmission scheduling mechanism for the cognitive internet of things," *IEEE Internet of Things Journal*, vol. PP, no. 99, pp. 1–1, 2017.

[9] A. C. Cirik, N. M. Balasubramanya, and L. Lampe, "Multi-user detection using ADMM-based compressive sensing for uplink grant-free NOMA," *IEEE Wireless Commun. Lett.*, vol. PP, no. 99, pp. 1–1, Sep. 2017.

[10] T. Qi, W. Feng, Y. Chen, and Y. Wang, "When NOMA meets sparse signal processing: Asymptotic performance analysis and optimal sequence design," *IEEE Access*, vol. 5, pp. 18 516–18 525, Jul. 2017.

[11] B. Tomasi, F. Gabry, V. Bioglio, I. Land, and J. C. Belfiore, "Low-complexity receiver for multi-level polar coded modulation in non-orthogonal multiple access," in *Proc. IEEE WCNC'17, San Francisco, CA, USA*, Mar. 2017, pp. 1–6.

[12] Z. Yang, Y. Luo, and L. Cai, "Network modulation: A new dimension to enhance wireless network performance," in *Proc. IEEE INFOCOM'11, Shanghai, China*, Apr. 2011, pp. 2786–2794.

[13] Z. Tang, J. Wang, J. Wang, and J. Song, "A low-complexity detection algorithm for uplink NOMA system based on gaussian approximation," in *Proc. IEEE WCNC'17, San Francisco, CA, USA*, Mar. 2017, pp. 1–6.

[14] Z. Yang, Z. Ding, P. Fan, and N. Al-Dhahir, "A general power allocation scheme to guarantee quality of service in downlink and uplink NOMA systems," *IEEE Trans. Wireless Commun.*, vol. 15, no. 11, pp. 7244–7257, Nov. 2016.

[15] J. Zhu, J. Wang, Y. Huang, S. He, X. You, and L. Yang, "On optimal power allocation for downlink non-orthogonal multiple access systems," *IEEE J. Sel. Areas Commun.*, vol. 35, no. 12, pp. 2744–2757, 2017.

[16] J. Choi, "On the power allocation for MIMO-NOMA systems with layered transmissions," *IEEE Trans. Wireless Commun.*, vol. 15, no. 5, pp. 3226–3237, May 2016.

[17] B. Di, L. Song, and Y. Li, "Sub-channel assignment, power allocation, and user scheduling for non-orthogonal multiple access networks," *IEEE Trans. Wireless Commun.*, vol. 15, no. 11, pp. 7686–7698, Nov. 2016.

[18] D. Zhai and J. Du, "Spectrum efficient resource management for multi-carrier based NOMA networks: A graph-based method," *IEEE Wireless Communications Letters*, vol. PP, no. 99, pp. 1–1, 2017.

[19] F. Fang, H. Zhang, J. Cheng, and V. C. M. Leung, "Energy-efficient resource allocation for downlink non-orthogonal multiple access network," *IEEE Trans. Commun.*, vol. 64, no. 9, pp. 3722–3732, Sep. 2016.

[20] X. Li, C. Li, and Y. Jin, "Dynamic resource allocation for transmit power minimization in OFDM-based NOMA systems," *IEEE Communications Letters*, vol. 20, no. 12, pp. 2558–2561, Dec. 2016.

[21] F. Fang, H. Zhang, J. Cheng, S. Roy, and V. C. M. Leung, "Joint user scheduling and power allocation optimization for energy efficient NOMA systems with imperfect CSI," *IEEE J. Sel. Areas Commun.*, vol. 35, no. 12, pp. 2874–2885, 2017.

[22] L. Lei, D. Yuan, C. K. Ho, and S. Sun, "Power and channel allocation for non-orthogonal multiple access in 5G systems: Tractability and computation," *IEEE Trans. Wireless Commun.*, vol. 15, no. 12, pp. 8580–8594, Dec. 2016.

[23] M. S. Ali, H. Tabassum, and E. Hossain, "Dynamic user clustering and power allocation for uplink and downlink non-orthogonal multiple access (NOMA) systems," *IEEE Access*, vol. 4, pp. 6325–6343, Aug. 2016.

[24] W. Liang, Z. Ding, Y. Li, and L. Song, "User pairing for downlink non-orthogonal multiple access networks using matching algorithm," *IEEE Trans. Commun.*, vol. 65, no. 12, pp. 5319–5332, 2017.

[25] L. Shi, B. Li, and H. Chen, "Pairing and power allocation for downlink non-orthogonal multiple access systems," *IEEE Trans. Veh. Technol.*, vol. 66, no. 11, pp. 10 084–10 091, 2017.

[26] J. Choi, "Joint rate and power allocation for noma with statistical CSI," *IEEE Trans. Commun.*, vol. 65, no. 10, pp. 4519–4528, Oct. 2017.

[27] W. Bao, H. Chen, Y. Li, and B. Vucetic, "Joint rate control and power allocation for non-orthogonal multiple access systems," *IEEE J. Sel. Areas Commun.*, vol. 35, no. 12, pp. 2798–2811, 2017.

[28] M. Mollanoori and M. Ghaderi, "Uplink scheduling in wireless networks with successive interference cancellation," *IEEE Trans. Mobile Comput.*, vol. 13, no. 5, pp. 1132–1144, May 2014.

[29] A. E. Mostafa, Y. Zhou, and V. W. S. Wong, "Connectivity maximization for narrowband IoT systems with NOMA," in *Proc. IEEE ICC'17, Paris, France*, May 2017, pp. 1–6.

[30] X. Wang and L. Cai, "Proportional fair scheduling in hierarchical modulation aided wireless networks," *IEEE Trans. Wireless Commun.*, vol. 12, no. 4, pp. 1584–1593, Apr. 2013.

[31] R. Zhang, R. Ruby, J. Pan, L. Cai, and X. Shen, "A hybrid reservation/contention-based MAC for video streaming over wireless networks," *IEEE J. Sel. Areas Commun.*, vol. 28, no. 3, pp. 389–398, Apr. 2010.

[32] L. Liu, X. Cao, W. Shen, Y. Cheng, and L. Cai, "DAFEE: a decomposed approach for energy efficient networking in multi-radio multi-channel wireless networks," in *Proc. IEEE INFOCOM'16, San Francisco, CA, USA*, Apr. 2016, pp. 1–9.

[33] J. Chen, K. Hu, Q. Wang, Y. Sun, Z. Shi, and S. He, "Narrowband internet of things: Implementations and applications," *IEEE Internet of Things Journal*, vol. 4, no. 6, pp. 2309–2314, Dec. 2017.

[34] R. Zhang, X. Lu, J. Zhao, L. Cai, and J. Wang, "Measurement and modeling of angular spreads of three-dimensional urban street radio channels," *IEEE Trans. Veh. Technol.*, vol. 66, no. 5, pp. 3555–3570, May 2017.

[35] R. Zhang, Y. Zhou, X. Lu, C. Cao, and Q. Guo, "Antenna deembedding for mmwave propagation modeling and field measurement validation at 73 GHz," *IEEE Trans. Micro. Theory Tech.*, vol. 65, no. 10, pp. 3648–3659, Oct. 2017.

[36] F. S. Chu, K. C. Chen, and G. Fettweis, "Green resource allocation to minimize receiving energy in OFDMA cellular systems," *IEEE Commun. Lett.*, vol. 16, no. 3, pp. 372–374, Mar. 2012.

[37] Z. Hasan, H. Boostanimehr, and V. K. Bhargava, "Green cellular networks: A survey, some research issues and challenges," *IEEE Commun. Surveys Tuts.*, vol. 13, no. 4, pp. 524–540, Nov. 2011.

[38] M. J. Neely, *Stochastic Network Optimization with Application to Communication and Queueing Systems*. Morgan & Claypool, 2010.

[39] S. Boyd and L. Vandenberghe, *Convex Optimization*. Cambridge University Press, 2004.

[40] D. Bertsekas and R. Gallager, *Data Networks*. Prentice-Hall, 1987.

[41] M. Neely, "Dynamic optimization and learning for renewal systems," *IEEE Trans. Autom. Control*, vol. 58, no. 1, pp. 32–46, Jan. 2013.

[42] S. Boyd and J. Mattingley, "Branch and bound methods," *Notes for EE364b, Stanford University*, 2007.

[43] D. Zhai, M. Sheng, X. Wang, Z. Sun, C. Xu, and J. Li, "Energy-saving resource management for D2D and cellular coexisting networks enhanced by hybrid multiple access technologies," *IEEE Trans. Wireless Commun.*, vol. 16, no. 4, pp. 2678–2692, Apr. 2017.

Daosen Zhai received the B.E. degree in telecommunication engineering from Shandong University, Weihai, China, in 2012, and the Ph.D. degree in communication and information systems from Xidian University, Xi¡¯an, China, in 2017. He is currently an assistant professor with the School of Electronics and Information, Northwestern Polytechnical University. His research interests focus on radio resource management in energy harvesting networks and 5G networks, topology control and connectivity analysis in ad hoc networks, and convex optimization and graph theory and their applications in wireless communications.

Ruonan Zhang (S'09-M'10) received his B.S. and M.Sc. degrees from Xi'an Jiaotong University, China, in 2000 and 2003, respectively, and Ph.D. degree from University of Victoria, BC, Canada, in 2010, all in electrical and electronics engineering. He worked as an IC architecture engineer at Motorola Inc. and Freescale Semiconductor Inc. in Tianjin, China, from 2003 to 2006. Since 2010, he has been with the Department of Communication Engineering at Northwestern Polytechnical University, Xi'an, Shaanxi, China, and he is currently a Professor. His research interests include wireless channel measurement and modeling, architecture and protocol design of wireless networks, and satellite communications. He has been a recipient of New Century Excellent Talent Grant from Ministry of Education of China, and the best paper award of IEEE NaNA 2016. He has served as a Local Arrangement Co-chair for IEEE/CIC International Conference on Communications in China (ICCC) 2013 and an associate editor for the Journal of Communications and Networks (JCN).

Lin Cai (S'00-M'06-SM'10) received her M.A.Sc. and Ph.D. degrees in electrical and computer engineering from the University of Waterloo, Waterloo, Canada, in 2002 and 2005, respectively. Since 2005, she has been with the Department of Electrical and Computer Engineering at the University of Victoria, and she is currently a Professor. Her research interests span several areas in communications and networking, with a focus on network protocol and architecture design supporting emerging multimedia traffic over wireless, mobile, ad hoc, and sensor networks.

She has been a recipient of the NSERC Discovery Accelerator Supplement Grant in 2010 and 2015, respectively, and the best paper awards of IEEE ICC 2008 and IEEE WCNC 2011. She has served as a TPC symposium co-chair for IEEE Globecom'10 and Globecom'13, the Distinguished Lecturer of the IEEE Vehicular Technology Society, and the Associate Editor for IEEE Transactions on Wireless Communications, IEEE Transactions on Vehicular Technology, EURASIP Journal on Wireless Communications and Networking, International Journal of Sensor Networks, and Journal of Communications and Networks (JCN).

Bin Li received his B.S. and Ph.D. degrees from Xi'an Jiaotong University, China, in 2006 and 2014, respectively, all in electrical and electronics engineering. Since 2014, he has been with the Department of Communication Engineering at the Northwestern Polytechnical University, Xi'an, Shaanxi, China, and he is currently a associate Professor. His current research interests include internet of things, network coding, MIMO, and wireless channel measurement modeling.

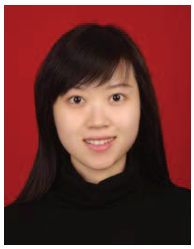

Yi Jiang received the B.E. degree in communication engineering form Northwestern Polythechnical University, Xi'an, China, in 2002, and the M.S. degree and Ph.D. degree in communication and information system from Northwestern Polythechnical University, Xi'an, China, in 2005 and 2008, respectively. She is currently an Associate Professor of communication and information system with Northwestern Polythechnical University, Xi'an, China. Her research interests include wireless networks, sensor networks, ad hoc networks, network security, RFID systems.